THE JOURNAL OF BIOLOGICAL CHEMISTRY
Vol. 279, No. 25, Issue of June 18, pp. 26323–26330, 2004

Printed in U.S.A.

Role of RhoA, mDia, and ROCK in Cell Shape-dependent Control of the Skp2-p27^{kip1} Pathway and the G_1/S Transition*

Received for publication, March 10, 2004, and in revised form, April 15, 2004
Published, JBC Papers in Press, April 19, 2004, DOI 10.1074/jbc.M402725200

Akiko Mammoto, Sui Huang, Kimberly Moore, Philmo Oh, and Donald E. Ingber‡

From the Vascular Biology Program, Departments of Pathology and Surgery, Children's Hospital/Harvard Medical School, Boston, Massachusetts 02115

Cell shape-dependent control of cell-cycle progression underlies the spatial differentials of growth that drive tissue morphogenesis, yet little is known about how cell distortion impacts the biochemical signaling machinery that is responsible for growth control. Here we show that the Rho family GTPase, RhoA, conveys the "cell shape signal" to the cell-cycle machinery in human capillary endothelial cells. Cells accumulating p27^{kip1} and arrested in mid G_1 phase when spreading were inhibited by restricted extracellular matrix adhesion, whereas constitutively active RhoA increased expression of the F-box protein Skp2 required for ubiquitination-dependent degradation of p27^{kip1} and restored G_1 progression in these cells. Studies with dominant-negative and constitutively active forms of mDia1, a downstream effector of RhoA, and with a pharmacological inhibitor of ROCK, another RhoA target, revealed that RhoA promoted G_1 progression by altering the balance of activities between these two downstream effectors. These data indicate that signaling proteins such as mDia1 and ROCK, which are thought to be involved primarily in cytoskeletal remodeling, also mediate cell growth regulation by coupling cell shape to the cell-cycle machinery at the level of signal transduction.

Formation of tissue patterns, such as branching capillary networks, requires that local spatial differentials of cell proliferation be established through the interplay between soluble growth factors, insoluble extracellular matrix (ECM)[1] molecules, and local changes in ECM mechanics that alter cell and cytoskeletal structure (1). Previous studies have demonstrated that cell-cycle progression can be controlled in the presence of soluble mitogens and ECM by altering physical interactions between cells and the ECM: substrates that prevent cell spreading inhibit proliferation, whereas those that support cell extension permit cell-cycle progression (2–4). ECM-dependent control of the shape of capillary endothelial cells, as well as other cells, can modulate the sensitivity of the cell to soluble growth factors (4–9). This shape-dependent growth control allows neighboring cells to undergo distinct cell fate transitions, a prerequisite for the generation of specialized tissue patterns (1, 10).

Cell spreading is an active process that is mediated by the binding of cell surface integrin receptors to ECM molecules and associated tension-dependent rearrangements of the actin cytoskeleton (11–14). Both cell spreading and maintenance of integrity of the actin cytoskeleton are required for endothelial cells or fibroblasts to complete the G_1 phase of the cell cycle and enter S phase (6, 15–18). Past work on the requirement of an intact cytoskeleton for growth control focused on early G_1 events, notably those mediated by the MAPK/Erk pathway (19–21). However, when endothelial cells are prevented from spreading by culturing them in the presence of soluble mitogens on dishes coated with a low density of the ECM protein fibronectin (FN) or on small, micrometer-sized, high density FN islands that are surrounded by non-adhesive regions, the G_1/S transition is similarly inhibited, despite normal activation of the canonical MAPK/Erk pathway (6). Cytoskeletal disruption also can prevent G_1 progression in many other cell types (16, 22–24). Thus, additional signals that emanate from the intact cytoskeleton of spread cells in mid-G_1 seem to be critical for the successful passage through late G_1 and entry into S phase (17, 18). However, virtually nothing is known about how distortion of the cell and cytoskeleton impact the biochemical signaling machinery that is responsible for this control of mid-late G_1 progression.

Cell-cycle progression through the late G_1/S restriction point, which represents the "point of no return" in the cell cycle, is associated with the hyperphosphorylation of retinoblastoma protein (pRb) by cyclin-dependent kinases (cdks) (17, 25–28). Notably, the cdk inhibitor p27^{kip1} (p27) that binds and inactivates the cyclin D1/cdk4 and cyclin E/cdk2 complexes is a major target for many physiological growth regulatory signals (29). Importantly, p27 levels remain high, and cell-cycle progression is blocked in mid- to late G_1 when endothelial cell spreading is prevented by either altering the ECM substrate or disrupting the actin cytoskeleton using various cytoskeletal modulators that act by means of distinct mechanisms (6). The effects of cell shape on cell-cycle progression are similarly mediated by p27 in other cell types (30–33). Thus, to understand the molecular basis of cell shape-dependent growth control, we must elucidate how cell spreading controls the level of this critical cell-cycle inhibitory protein.

Skp2, a member of the family of proteins that contain an F-box motif (34), is part of the Skp2, Cul1, and F-box protein complex which is responsible for degradation of various cell-cycle proteins. Availability of the Skp2 subunit is rate-limiting, and it directly regulates ubiquitination and the subsequent degradation of phosphorylated p27 *in vitro* and *in vivo* (35–38).

* This work was supported by National Institutes of Health Grant CA58833 (to D. E. I.) and a Toyobo postdoctoral fellowship (to A. M.). The costs of publication of this article were defrayed in part by the payment of page charges. This article must therefore be hereby marked "*advertisement*" in accordance with 18 U.S.C. Section 1734 solely to indicate this fact.

‡ To whom correspondence should be addressed: Vascular Biology Program, Departments of Pathology & Surgery, Children's Hospital/Harvard Medical School, Room 11–127, Karp Family Research Laboratories, 300 Longwood Ave., Boston, MA 02115. Tel.: 617-919-2223; Fax: 617-730-0230; E-mail: donald.ingber@childrens.harvard.edu.

[1] The abbreviations used are: ECM, extracellular matrix; FN, fibronectin; pRb, retinoblastoma protein; cdks, cyclin-dependent kinases; p27, p27^{kip1}; ROCK, rho-associated kinase; mDia, mDia1; RT, reverse transcription; CNF1, cytotoxic necrotizing factor 1; GST, glutathione *S*-transferase; SRF, serum response factor.

Skp2 has been shown to play a role in cell-cycle control by signals elicited by both growth factor receptors and integrins (33). However, in past studies using micropatterned ECM islands that allowed us to dissociate signals elicited by direct integrin binding from cell spreading, we showed that integrin-mediated adhesion to ECM and subsequent changes of cell shape convey distinct growth signals to the cell-cycle machinery, and that cell spreading is a critical determinant of p27 levels in these cells (1, 4, 6). Thus, Skp2 is a potential candidate for mediating the effects of cell shape on p27, but there is still no known link between cytoskeletal distortion and Skp2.

Small GTPase proteins, including RhoA, Rac1, and cdc42, are interesting candidates for linking cell shape and cell-cycle progression because of their role in both cytoskeletal arrangements and mitogenic signaling. These small G proteins regulate a multitude of cellular functions including cell adhesion, focal adhesion formation, cytoskeletal remodeling, spreading, motility, polarization, and cytokinesis by ligation of growth factor receptors and integrin receptors, as well as by mechanical stresses (39–45). Rho family proteins also play critical roles in cell-cycle progression through G_1 phase (46–50). Signals elicited by integrin binding decrease p27 levels and promote synthesis of cyclin D1; moreover, these effects seem to be mediated by Rac1 and cdc42 (49–51). RhoA also has been reported to down-regulate both $p21^{cip1}$ and p27 and to stimulate cyclin D1 accumulation in various settings (20, 52–58). However, the downstream targets of RhoA that link it with the cell-cycle machinery remain elusive.

Because of its dual roles in integrin-mediated actin-cytoskeletal rearrangements during cell spreading and in control of G_1 progression, the Rho signaling pathway is a prime candidate for mediating cell shape-dependent cell-cycle regulation. Two well studied downstream effectors of RhoA, rho-associated kinases (ROCK) and the formin homology protein mDia1 (mDia) have emerged as the chief mediators of the effect of Rho on the actin cytoskeleton. ROCK stimulates actomyosin-based cell contractility by promoting myosin light chain phosphorylation and increases cytoskeletal tension that is necessary for formation of focal adhesions and stress fibers (59, 60). In contrast, mDia promotes actin polymerization (61), mediates the effects of external mechanical stresses on actin-dependent focal adhesion formation (62), and regulates alignment of stress fibers with microtubules by targeting microtubules to focal adhesions (63–65). ROCK and mDia seem to act jointly in controlling cytoskeletal rearrangements to provide a scaffold for the stabilization of a normal cell shape (62, 63); however, ROCK and mDia activities also may antagonize each other in cell shape control, or in the formation of membrane ruffles and adherens junctions (66–68). But these studies of RhoA effector functions were largely limited to their structural effects; their role in cell-cycle progression has yet to be elucidated.

Here we demonstrate that RhoA mediates cell shape-dependent cell-cycle progression in human microvascular endothelial cells. Our data show that RhoA acts downstream of cell spreading to promote G_1 progression by activating the Skp2-$p27^{kip1}$ pathway, and that its effects are mediated, in part, by a balance between the activities of its two downstream signaling targets, mDia and ROCK.

EXPERIMENTAL PROCEDURES

Cell Culture—Human microvascular endothelial cells from neonatal dermis (Cascade Biologics, Portland, OR) were cultured in EBM-2 (Cascade Biologics), supplemented with 5% fetal bovine serum and growth factors (basic fibroblast growth factor, insulin-like growth factor, vascular endothelial growth factor) according to the manufacturer's instructions. Cells were synchronized at the G_0/G_1 border by serum starvation (0.3% fetal bovine serum/EBM-2) for 40–42 h and then released into G_1 by trypsinizing the cells and replating them on FN-coated dishes in EBM-2 containing 1% fetal bovine serum and growth factors.

Experimental System—To control cell shape, cells were cultured on bacteriological Petri dishes (35-mm Petri dishes; Falcon, Lincoln Park, NJ) that were pre-coated with different densities (22 ng/cm^2 or 666 ng/cm^2) of FN (Collaborative Biomedical Products, Bedford, MA) using a carbonate buffer-coating technique, as described previously (3, 6). For morphological analysis, cells were fixed for 10 min in 4% paraformaldehyde/PBS, incubated for 5 min in 0.3% Triton X-100/PBS, and then blocked overnight with 0.5% bovine serum albumin/PBS. Focal adhesions were visualized using anti-paxillin monoclonal antibody (Transduction Laboratories, Lexington, KY). F-actin was visualized using Alexa-488 phalloidin (Sigma). In the study examining the morphological effect of mDia978 on Y27632-treated cells, 5 μM lysophosphatidic acid (Sigma) was used in place of serum, as described previously (68).

Cell-cycle Analysis—Cell cycle-associated proteins were detected by Western blotting and reverse transcription (RT)-PCR as described previously (6). In these studies, cells cultured on 60-mm dishes were lysed with 0.3 ml of boiling lysis buffer (1% SDS, 50 mM Tris-HCl, pH 7.4) and scraped, and lysates were collected (6). Homogenized total cell lysates (10 μg protein) were subjected to SDS-PAGE, transferred to nitrocellulose membrane, and immunoblotted with specific primary antibodies. The primary antibodies were detected using horseradish peroxidase-conjugated secondary antibodies (Vector Laboratories, Burlingame, CA) and SuperSignal Ultra (Pierce) as a chemiluminescence substrate. Monoclonal antibodies directed against the following antigens were obtained from these suppliers: pRb (LM95.1) from Calbiochem (San Diego, CA), Skp2 (SKP2–8D9) from Zymed Laboratories Inc. (San Francisco, CA), and actin (AC-15) from Sigma. Polyclonal antibody against $p27^{kip1}$ (clone 57) was purchased from Santa Cruz Biotechnologies (Santa Cruz, CA). Y27632 was purchased from Calbiochem. Results were quantified by densitometric analysis using NIH image software. The Mann-Whitney *U* test was used for analysis of statistical significance of replicate Western blots.

RT-PCR was used to determine the expression of Skp2 mRNA. Adherent cells were lysed and total RNA was isolated using the RNeasy RNA extraction kit (Qiagen, Valencia, CA). The RNA (500 ng/sample) was treated for 1 h at 37 °C with reverse transcriptase using OmniScript reverse transcriptase assay kit (Qiagen). The PCR was carried out with a series of 1:3 dilutions of the RT product (2 μl). Only reactions in the log-linear range (product quantity *versus* input template quantity) were used. The forward and reverse PCR primers for Skp2 were 5′-CAACTACCTCCAACACCTATC-3′ and 5′-TCCTGCCTATTTTCCCTGTTCT-3′, respectively. PCR cycling conditions were 3 min at 94 °C, then 26 cycles of 30 s at 94 °C, 30 s at 62 °C, and 1 min at 72 °C. For internal control, we used β actin mRNA, whose forward and reverse primers were 5′-TGACGGGGTCACCCACACTGTGCC-3′ and 5′-TAGAAGCATTTGCGGTGGACGATG-3′, respectively. PCR products were analyzed by agarose gel electrophoresis. Primers were designed with Oligo version 4.0 software (National Biosciences, Plymouth, MN) and synthesized by Sigma Genosys (Biotechnologies Industries, The Woodlands, TX).

Preparation of Recombinant Proteins—The constitutively active form of RhoA (RhoA14V) and cytotoxic necrotizing factor 1 (CNF1) were expressed and purified from *Escherichia coli* expression plasmid pGEX4T-RhoA14V and pCNF24-CNF1 (kindly provided by Alan Hall, University College London, UK, and Melody Mills, Uniformed Services University of the Health Sciences, Bethesda, MD, respectively). The plasmids encoding full-length mDia were kindly provided by Yoshimi Takai (Osaka University, Japan). The dominant-negative form of mDia (mDia978, amino acids 543–978) and the constitutively active form of mDia (mDia1192, amino acids 543–1192) were constructed using PCR and subcloned into the glutathione *S*-transferase (GST)-fusion protein/*E. coli* expression vector pGEX4T-1 (Amersham Biosciences) at the EcoRI/XhoI and BamHI/XhoI sites, respectively. GST-tagged RhoA14V, mDia978, and mDia1192, as well as GST recombinant proteins, were purified from *E. coli*, as previously described (69). For RhoA14V, the GST tag was removed by proteolytic cleavage with thrombin (10 units/ml, Sigma) at 4 °C for 8–10 h; thrombin was removed by incubating the supernatant with *p*-amino-benzamidine-agarose (Sigma). Because of the presence of multiple thrombin target sites, the GST fragment could not be cleaved away from the mDia fusion protein. The His-tagged CNF1 was purified with Ni-agarose nitrilotriacetic acid beads following the manufacturer's instructions (Qiagen). C3 exoenzyme was purchased from Cytoskeleton Inc. (Denver, CO).

Protein Transfection—For protein transfection (proteofection), we used BioPORTER protein delivery reagent (Gene Therapy Systems, San Diego, CA) according to the manufacturer's instructions. In brief,

0.5–5 μg of recombinant protein in 200 μl of PBS was incubated in a tube containing a film of 15 μl of BioPORTER that was formed by drying for 5 min. The complexes were then added to the cells (400,000 cells/60-mm dish) in 2.5 ml of serum-free EBM-2; after 4 h of incubation at 37 °C, cells were replated onto the experimental FN-coated dishes with experimental medium. In the case of RhoA14V and C3, we used the BioPORTER reagent alone without added protein cargo as a proteofection control. In the case of mDia978 and mDia1192, which contained a GST sequence, we proteofected the GST portion of the protein as a control. The samples were collected at the indicated time points after replating.

RESULTS

FN Density-dependent Control of Capillary Cell Shape and G_1 Progression—We demonstrated previously that pulmonary capillary endothelial cell spreading and growth can be controlled in parallel by culturing the cells on dishes coated with different molecular coating densities of the ECM protein, FN (6). Experiments were first carried out to confirm the generality of this behavior by demonstrating that cell shape and progression through the G_1/S transition can be similarly controlled in microvascular endothelial cells from human neonatal dermis. The levels of the critical G_1 protein, p27, were measured in total cell lysates; the phosphorylation status of pRb was used as a read-out of successful progression through the late G_1 restriction point. Cells synchronized in G_0 by serum starvation were replated on dishes coated either with a high density (666 ng/cm^2) of FN (high FN) that allows maximal cell spreading, or with a low density (22 ng/cm^2) of FN (low FN), on which cells attach but remain retracted or round. Western blot analysis confirmed that the levels of hyperphosphorylated pRb increased and p27 decreased, as the spread cells on high FN progressed from G_0 (time 0) to late G_1 phase (from 8 to 18 h after release) (Fig. 1). In contrast, round cells on low FN did not down-regulate p27 or hyperphosphorylate pRb over the same time course, even though they were stimulated by the same soluble mitogens (basic fibroblast growth factor, insulin-like growth factor, and vascular endothelial growth factor in 1% serum) (Fig. 1). These results confirm that cell spreading is necessary to promote passage through the G_1/S restriction point in human dermal capillary endothelial cells, just as it is in human pulmonary capillary cells (6) and in bovine endothelial cells from both small and large vessels (3, 10).

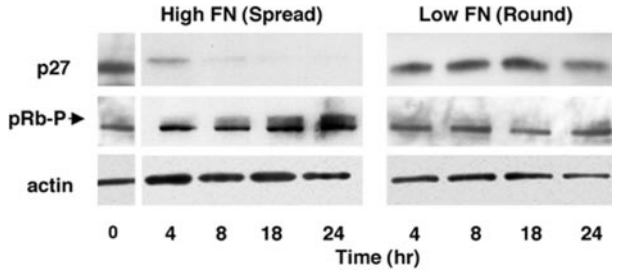

FIG. 1. **FN density-dependent control of cell spreading regulates G_1 progression in human dermal capillary endothelial cells.** Immunoblots showing changes in the level of expression of p27 proteins relative to β actin, as well as Rb protein phosphorylation status, in total cell lysates from spread and round cells cultured on high and low FN, respectively, for the indicated times after release from G_0. For pRb, the slower-migrating (*top*) band represents the hyperphosphorylated form of the protein.

RhoA Mediates Shape-dependent Growth Control—To explore the role of RhoA in shape-dependent cell-cycle control, we used genetically modified recombinant RhoA proteins and toxins to specifically activate or inhibit Rho activity. We used proteofection techniques that provide greater than 95% transfection efficiency and permit much better temporal control of signaling activities than plasmid transfection. To confirm that these agents were active in capillary cells using this method, we first analyzed their effects on cell morphology and the actin

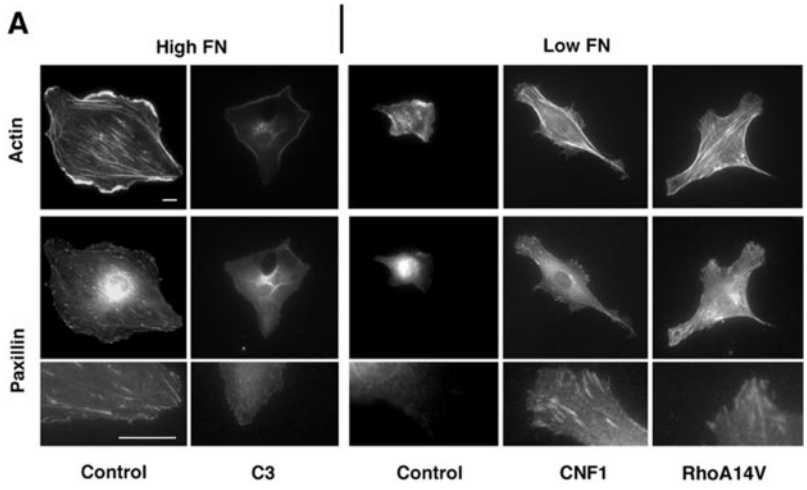

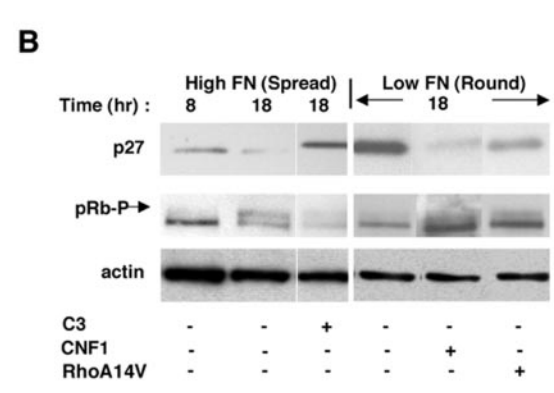

FIG. 2. **RhoA mediates cell shape-dependent control of G_1 progression.** *A*, fluorescence micrographs showing control of cell shape, stress fiber formation, and focal adhesion assembly by C3, CNF-1, and RhoA14V in spread *versus* round cells on high *versus* low FN. F-actin was visualized by staining with Alexa-488 phalloidin; focal adhesions were stained with an anti-paxillin antibody (*bar* = 5 μm). *B*, immunoblots showing control of p27 and pRb phosphorylation by C3, CNF-1, and RhoA14V in spread *versus* round cells at the indicated times after release from G_0.

cytoskeleton (Fig. 2*A*). As previously documented for fibroblasts (39–41), the well defined stress fibers and focal adhesions that appeared in highly spread cells on high FN were lost when cells were proteofected with the specific Rho-inhibiting toxin, C3 exoenzyme (70). Round cells on low FN also failed to exhibit either stress fibers or detectable focal adhesions. Conversely, treatment of these round cells with CNF1 (100 ng/ml), a toxin that activates all Rho family GTPases (71–73), or proteofection with constitutively active RhoA (RhoA14V) protein was able to induce formation of both well defined stress fibers and focal adhesions on low FN. Interestingly, RhoA activation also induced a significant increase in cell spreading ($p < 0.001$) in these cells when quantitated by computerized morphometry. These findings indicate that RhoA activity may be able to reconstitute some structural features of spread cells within cells on low FN despite constant external constraints on integrin binding and cell extension because of the low availability of FN binding sites.

To explore whether RhoA contributes to shape-dependent growth control, G_0-synchonized cells were plated in the presence of serum and growth factors on a low or high FN density in the presence or absence of the different RhoA modulators, and cell-cycle proteins were monitored 8 h (early G_1) and 18 h (late G_1) later. The delivery of C3 exoenzyme by proteofection into spread cells on high FN inhibited pRb hyperphosphorylation and led to abnormal accumulation of p27 (Fig. 2*B*), as observed previously in other cell types (53, 56). Importantly, proteofection of round cells on low FN with active RhoA or treatment with CNF1 was able to down-regulate p27 and induce passage through the late G_1 restriction point, as measured by pRb hyperphosphorylation (Fig. 2*B*). These results demonstrate that RhoA is sufficient to overcome the late G_1 cell-cycle block imposed by cell rounding, and suggest that RhoA may normally act downstream of signals produced by cell spreading on ECM to promote cell-cycle progression.

Cell Spreading Up-regulates Skp2 Expression in Late G_1 Phase through Activation of RhoA—The F-box protein Skp2 that stimulates ubiquitination and subsequent degradation of p27 (35–38) has been implicated in cell-cycle control by both growth factors and anchorage to ECM in fibroblasts (33). Because our past work suggests that anchorage-dependent growth control is largely based on regulation of G_1 progression by cell shape rather than ECM adhesion (*i.e.* integrin binding) *per se* (6), we therefore set out to explore whether Skp2 mediates the effects of cell spreading on p27 in human dermal microvascular cells. When G_0-synchronized cells were plated on high FN, Skp2 mRNA expression increased during G_1 progression, whereas it remained relatively low in the round cells on low FN (Fig. 3*A*). This inhibition of Skp2 expression in cells on low *versus* high FN was even more evident when the effects on Skp2 protein levels were analyzed (Fig. 3*A*).

To explore whether the effects of cell shape on Skp2 are mediated by RhoA, spread cells on high FN were proteofected with C3 exoenzyme. Inhibition of RhoA prevented the induction of Skp2 mRNA and protein in these spread cells, whereas ectopic activation of RhoA using RhoA14V was able to induce Skp2 expression levels in round cells (Fig. 3*B*). These results demonstrate that RhoA activity is required for Skp2 expression in normally spread cells, and that it is also sufficient to stimulate Skp2 expression in the absence of high FN and optimal cell spreading.

ROCK Activity Is Not Required for Cell Shape-dependent G_1 Progression—In past studies with other endothelial cells, the level of cytoskeletal tension in the cytoskeleton was found to partly contribute to shape-dependent control of cell-cycle regulation (6, 74). Thus, we examined whether ROCK, the RhoA

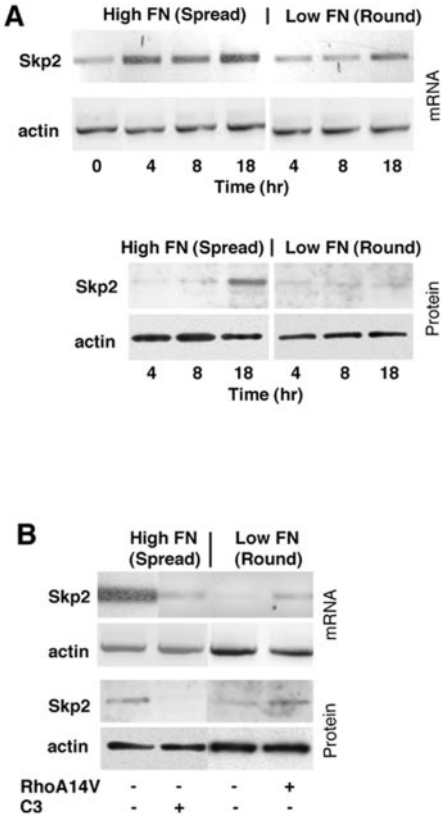

FIG. 3. **Control of Skp2 expression by cell shape and RhoA.** *A*, changes in the levels of expression of Skp2 mRNA (*top*) and protein (*bottom*) measured 0–18 h after release from G_0 by semi-quantitative RT-PCR and immunoblotting of total cell lysates, respectively, in cells on high *versus* low FN. *B*, effects of RhoA14V and C3 on the expression of Skp2 mRNA and protein in round *versus* spread cells. Samples were collected 18 h after release from G_0, which corresponds to late G_1 in these cells. As an internal control, β actin mRNA and protein levels were measured in parallel in both studies.

target that enhances cytoskeletal contractility, regulates cell-cycle progression in our dermal capillary endothelial cells using its specific inhibitor, Y27632. Treatment of spread cells on high FN with Y27632 (10 μM) resulted in a characteristic phenotype that has been described previously in other similarly treated cells: the cells remained spread and exhibited fewer focal adhesions and less stress fibers with thinner and more diffuse actin filaments, as well as increased formation of membrane ruffles (Fig. 4*A*; Refs. 68, 75). Increased ruffle formation was also observed in round cells on low FN (Fig. 4*A*). However, Y27632 failed to inhibit the down-regulation of p27 or pRb hyperphosphorylation that is normally observed in spread cells on high FN (Fig. 4*B*). In fact, we consistently found that Y27632 induced a moderate increase in Skp2, and a decrease in p27, in addition to promoting pRb hyperphosphorylation in round cells on low FN (Fig. 4*B*).

mDia Is Necessary for RhoA-stimulated G_1/S Transition—Although the results with Y27632 do not exclude a role for cell tension in cell shape-dependent growth control, they clearly dispel the possibility that ROCK is the main target through which RhoA exerts its stimulating effect on G_1 progression in these cells. Specifically, one caveat in the interpretation of our results with the ROCK inhibitor is that several reports have demonstrated a functional antagonism between ROCK and another downstream target of Rho, mDia1, with regard to their effects on actin filaments, ruffling formation, and junctional adhesions (66–68). Therefore, we carried out studies to determine whether mDia1 might convey cell shape-dependent signals to the cell-cycle machinery through its antagonism to

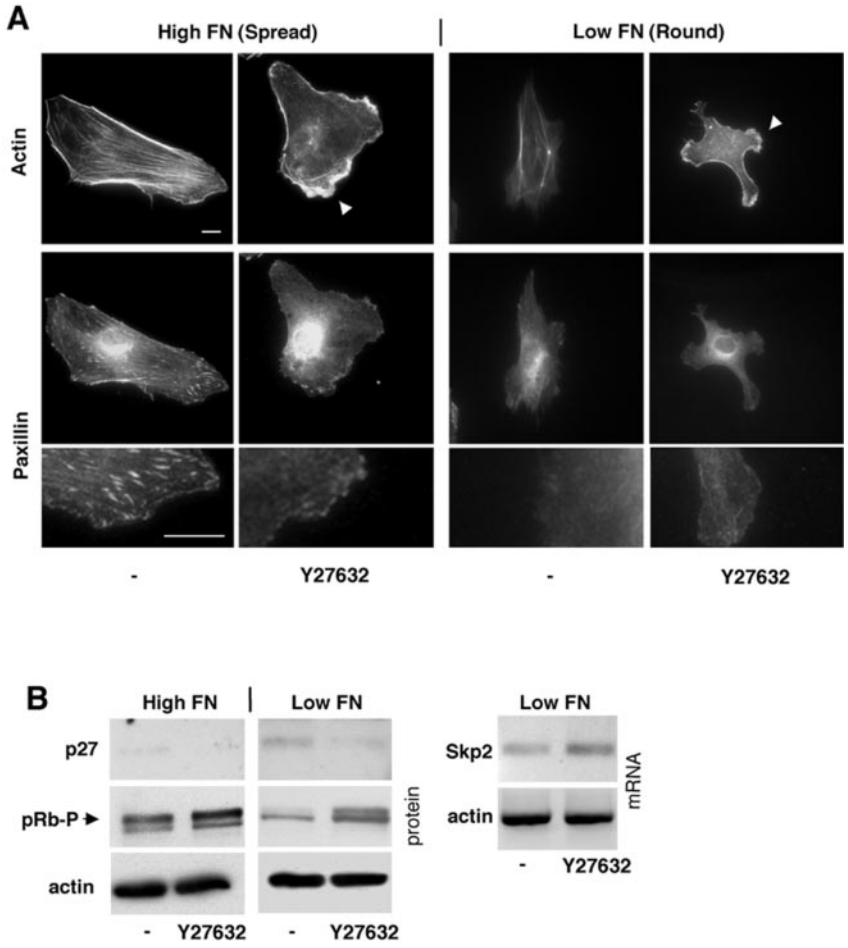

FIG. 4. **The ROCK inhibitor Y27632 alters cytoskeletal organization and induces release from arrest in late G_1.** *A*, fluorescence micrographs showing induction of membrane ruffle formation (*white arrowheads*) and inhibition of focal adhesion assembly and stress fiber formation by treatment of both spread and round cells with 10 μM Y27632 for 18 h after release from G_0 (*bar* = 5 μm). *B*, immunoblots showing the effects of Y27632 on p27 protein levels, pRb phosphorylation, and Skp2 mRNA levels in cells on high *versus* low FN. Samples were collected 18 h after release from G_0.

ROCK. In fact, although Y27632 induced ruffle formation in poorly spread cells on low FN, it failed to do so when cells were cotransfected with dominant-negative mDia (mDia978) protein (Fig. 5*A*). Thus, mDia1 seems to actively participate in cell shape regulation in these capillary endothelial cells by balancing the activity of endogenous ROCK.

Because ROCK-inhibition by Y27632 not only altered the cytoskeleton (Fig. 4*A*) but also stimulated passage through the G_1 restriction point in the absence of cell spreading (Fig. 4*B*), we examined whether this effect on the cell cycle also depended on release of previously masked mDia1 activity from the antagonism with ROCK. Transfection of dominant-negative mDia978 into Y27632-treated cells on low FN completely prevented the G_1-promoting effects of Y27632 (Fig. 5*B*, increase in Skp2, p27 down-regulation, rise in pRb hyperphosphorylation). Moreover, mDia978 also suppressed the ability of RhoA14V to rescue round cells from G_1 arrest on low FN by altering Skp2, p27, and pRb hyperphosphorylation (Fig. 5*C*). Analysis of results from three independent studies confirmed that all of these effects of mDia978 on p27 were statistically significant ($p < 0.05$). mDia1 is therefore required for RhoA- and ROCK-inhibition to activate the Skp2-p27 signaling cascade and trigger release from late G_1 arrest in round cells.

mDia Alone Is Not Sufficient to Promote G_1 Progression—A constitutively active, recombinant form of mDia, mDia1192, was proteofected into cells on low FN to determine whether mDia is sufficient to promote G_1 progression in round cells. The active form of mDia (mDia1192) did not significantly alter p27 or Skp2 mRNA levels (Fig. 5*D*). Thus, although mDia seems to be required for the effects of RhoA on G_1 progression in round cells, it is not the sole trigger for the Skp2 induction and p27 down-regulation that are necessary for passage through the late G_1

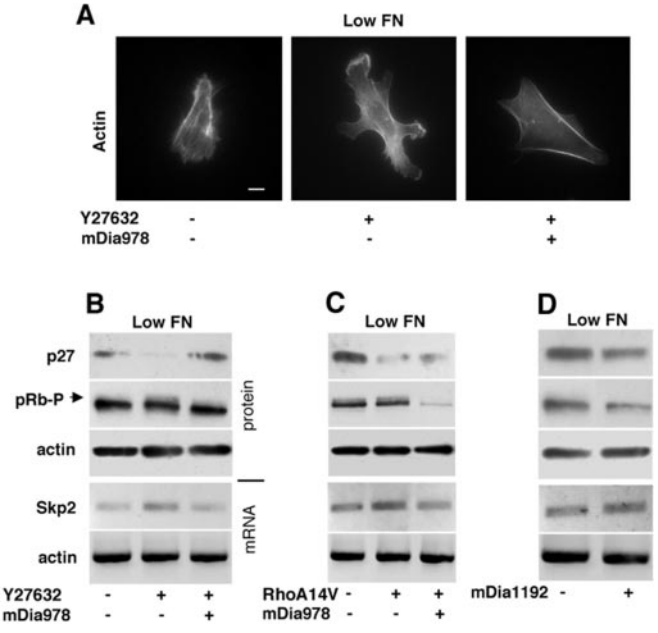

FIG. 5. **Evidence for control of cell-cycle progression by a balance between ROCK and mDia activities.** *A*, fluorescence micrographs showing induction of membrane ruffle formation by Y27632 and its inhibition by dominant-negative mDia978 (*bar* = 5 μm). *B*, immunoblots showing the effects of Y27632 in the absence or presence of mDia978 on p27 protein, pRb hyperphosphorylation, and Skp2 mRNA in round cells on low FN. *C*, immunoblots showing effects of RhoA14V in the absence or presence of mDia978 on the same cell cycle-associated molecules. *D*, immunoblots visualizing the cell-cycle effects of constitutively active mDia1192.

checkpoint. Other RhoA-dependent signaling events that may be masked by ROCK are also required for this response.

DISCUSSION

Regulation of cell cycle G_1 progression by cell spreading plays a central role in the spatial control of cell proliferation that is crucial for generation of tissue patterns during angiogenesis. Capillary endothelial cells must spread on ECM in order for mitogenic stimuli to promote their transition through the late G_1 restriction point and entry into S phase. However, little is known about how changes in cell shape influence the molecular players that drive the cell-cycle machinery. Here we demonstrate a role for RhoA and its downstream signaling components, including mDia and ROCK, in conveying the cell shape signal. Specifically, we showed that G_1 progression can be inhibited in spread capillary cells by suppressing the activity of RhoA or its downstream effector mDia1 which, in turn, decreases expression of the F-box protein Skp2 that controls a rate-limiting step in ubiquitin-mediated degradation of the critical cdk inhibitor, p27 (35–38). Importantly, our findings showed that ectopic RhoA activity was sufficient to rescue cells from G_1 arrest on substrates coated with low FN that normally prevent cell spreading and prohibit S phase entry. Tipping the balance between the two Rho effectors, mDia1 and ROCK, toward mDia1 similarly promoted G_1 progression under these conditions.

The critical role that RhoA plays in shape-dependent cell-cycle progression, in particular, its ability to substitute for signals generated by cell spreading, ostensibly seems to contradict a report in which Rho activity measured with a rhotekin-binding assay was found to be higher in suspended (round) *versus* attached (spread) cells (76). According to that report, active RhoA that is present in suspended cells becomes inactivated immediately after cells adhere to ECM, and then RhoA activity levels rise and are thereafter maintained at low levels. However, these sustained basal levels of RhoA are obviously essential functionally because our findings show that inhibition of RhoA in spread cells with C3 has dramatic effects on both cytoskeletal organization and cell-cycle progression. Moreover, quantitation of the activity of RhoA based solely on its ability to bind rhotekin may not necessarily reflect the activating potential of RhoA on its other targets (77) or its position in the cell.

What mediates the effects of RhoA on the cell-cycle machinery? Two downstream targets of RhoA, ROCK and mDia1, have emerged as the major effectors of the ability of RhoA to control cytoskeletal rearrangements and cell morphology. Here we demonstrate a new function for these effectors, in that they also play a central role in the control of the biochemical machinery that drives cell-cycle progression. Although ROCK and mDia cooperate to control integrated cytoskeletal functions, such as focal adhesion formation and cell shape stabilization (62, 63), they antagonize each other during the formation of stress fibers, cell-cell adherens junctions, and membrane ruffles (66–68). Our finding that the inhibition of ROCK by using Y27632 actually induces release from the late G_1 block in capillary cells is consistent with similar findings observed previously in fibroblasts (78). However, Y27632 did not affect p27 levels in those cells, whereas treatment of shape-restricted capillary cells on low FN with Y27632 induced Skp2 mRNA expression and thereby decreased p27 levels in the present study. This inconsistency may be due to the fact that we used different cell types and experimental conditions. But what is striking in our study is that inhibition of the Rho target ROCK can partially rescue round cells from G_1 arrest. Thus, ROCK inhibition produces the same net effect as stimulation of RhoA, its upstream activator.

How can this paradox be reconciled? Our results show that mDia and ROCK antagonize each other with regard to G_1/S transition in endothelial cells in the same way as has been shown for their effects on cytoskeletal remodeling in other cell types (66–68). The importance of a balance between these two RhoA effectors is supported by the following findings: (*i*) blocking ROCK with Y27632 induced morphological changes (*e.g.* ruffle formation) in our endothelial cells that have been previously associated with mDia1 activity in other cell types (66–68), and these morphological alterations could be inhibited by dominant-negative mDia (mDia978); and (*ii*) both Y27632 and constitutively active RhoA were able to rescue round cells from G_1 arrest by promoting p27 degradation, and these effects again were both inhibited by mDia978. Thus, when ROCK activity was inhibited, mDia1 activity became unopposed, and hence was functionally enhanced; this resulted in the promotion of mDia1-dependent G_1 progression (Fig. 6). Although mDia1 is necessary for shape-induced G_1 progression, transfection of constitutively active mDia (mDia1192) was not sufficient to promote G_1 progression in round cells. Thus, mDia may not be the only growth-promoting Rho effector that is kept in balance by ROCK. These other mitogenic signals may include Rac, as we have found that it is required for the rescue of G_1 arrest in round cells on low FN by both RhoA14V and ROCK inhibition with Y27632 (data not shown), and others have shown that it mediates membrane ruffle formation induced by Y27632 (68).

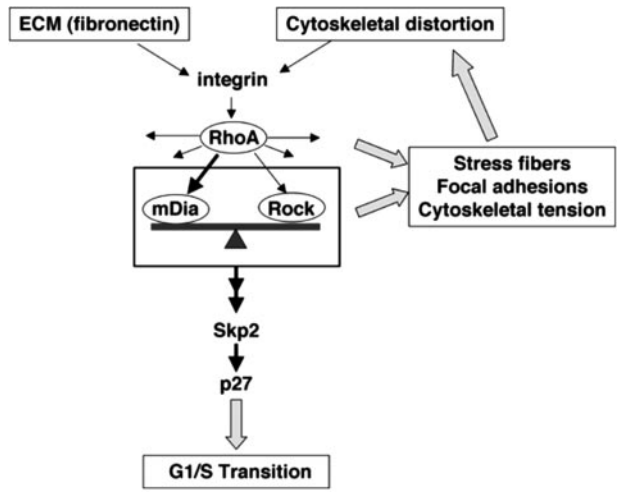

FIG. 6. **Schematic model of cell shape-dependent control of cell-cycle progression.** Integrin binding has been shown to initially inhibit RhoA activity during the first 30 min after cell attachment to ECM (76). Rho activity then rises and peaks 1 h after plating as the cell spreads; it then slowly declines to a low basal level over the following 6 h. This low level of RhoA signaling is necessary for stress fiber formation, focal adhesion assembly, and cytoskeletal tension generation through activation of the downstream effectors of RhoA, ROCK and mDia (RhoA also may promote cytoskeletal changes through other downstream effectors as well; Ref. 77). The increase in cell tractional forces feeds back to produce additional distortion of integrins and the cytoskeleton; this drives further cell flattening and spreading. This increase in the level of tension transmitted across integrins further activates mDia and ROCK (62), thereby producing more tension, and hence promotes additional formation of focal adhesions and stress fibers. However, mDia and ROCK also antagonize one another in terms of control of stress fiber formation, focal adhesion assembly, and induction of the F-box protein, Skp2. When mDia activity dominates, Skp2 protein and mRNA levels increase; this promotes ubiquitin-mediated degradation of the critical cdk inhibitor, p27, which then releases cells from late G_1 arrest and promotes cell-cycle progression.

Our results leaves a central question unanswered: if ROCK is inhibitory with respect to G_1 progression, whereas mDia is stimulatory, then why does RhoA promote G_1 progression, given that both are its downstream targets? Our data suggest that RhoA14V may preferentially activate mDia1 relative to ROCK, and thereby shift the balance toward mDia1 in our

capillary cells; this would produce a mitogenic effect similar to that induced by treatment with the ROCK inhibitor Y27632. In fact, there is indirect evidence based on C3 dose-response experiments that, at least with regards to cell morphology and migration, higher levels of RhoA activity are required to activate ROCK than mDia1 (79).

In this study, we demonstrated that Skp2-p27 pathway is regulated by RhoA. A recent report showed that Rho controls activity of the transcription factor serum response factor (SRF) by modulating actin dynamics and thereby altering nuclear accumulation of myocardin-related SRF coactivator (80). The same group also reported that mDia controls the SRF activity by means of actin polymerization (81). These findings are consistent with our observation that mDia stimulates Skp2 transcription in late G_1 and raise the possibility that this effect could be mediated by the myocardin-related SRF coactivator/SRF pathway.

Can a biochemical cascade, such as the Rho-mDia/ROCK-Skp2-p27 pathway, replace a "shape dependent" signal? Our results showing the regulation of G_1 progression in response to various perturbations indicate that cell-cycle progression restored by RhoA14V in round cells is not identical to the physiological signal provided by cell spreading. In more general terms, the various methods used to abrogate cell shape and reconstitute cytoskeletal signals are not equivalent, as they affect different sets of signaling pathways. For instance, G_1 progression can be arrested in various cell types by disrupting the actin cytoskeleton with cytochalasin D (6, 16, 18, 22, 82); however, RhoA, mDia1192, and Y27632 failed to restore pRb phosphorylation in cytochalasin D-treated capillary cells, even though they down-regulate p27 (data not shown). This is in direct contrast to our finding that RhoA14V fully restored G_1 progression in round cells on low FN, whereas it is reminiscent of the failure of active mDia to restore G_1 progression in round cells on low FN. Moreover, activation of RhoA also promoted a statistically significant, although subnormal, increase in cell spreading, as well as formation of both stress fibers and focal adhesions in cells on low FN. Thus, part of the growth-promoting effect of constitutively active RhoA may be conveyed by its effects on cell shape and the cytoskeleton (*i.e.* partial spreading). Taken together, these findings suggest a hierarchy of cytoskeletal- and shape-dependent mitogenic signals. For example, cytochalasin D may have more disrupting effects on cytoskeletal integrity than prevention of spreading by plating cells on low FN density. RhoA also seems to have more restoring power than its downstream target mDia, and it may effectively act both downstream and upstream of cell spreading in different contexts.

In summary, our work helps to translate the long-recognized phenomenon of cell shape-dependent growth control into detailed molecular terms. It establishes the importance of RhoA in cell shape-dependent G_1 progression and identifies mDia1, ROCK, Skp2, and p27 as key downstream effectors that link cell distortion to the cell-cycle machinery. The finding that mDia1, a signaling protein thought primarily to be involved in control of cytoskeletal remodeling, also regulates biochemical events involved in growth control opens up an entirely new avenue of investigation into the mechanism by which mechanical forces and cytoskeletal deformation can influence cellular biochemistry and gene expression.

Acknowledgments—We thank A. Hall, M. Mills, and Y. Takai for providing plasmids.

REFERENCES

1. Huang, S., and Ingber, D. E. (1999) *Nat. Cell. Bio.* **1,** E131–E138
2. Ingber, D. E., and Folkman, J. (1989) *J. Cell Biol.* **109,** 317–330
3. Ingber, D. E. (1990) *Proc. Natl. Acad. Sci. U. S. A.* **87,** 3579–3583
4. Chen, C. S., Mrksich, M., Huang, S., Whitesides, G. M., and Ingber, D. E. (1997) *Science* **276,** 1425–1428
5. Singhvi, R., Kumar, A., Lopez, G., Stephanopoulos, G. N., Wang, D. I. C., Whitesides, G. M., and Ingber, D. E. (1994) *Science* **264,** 696–698
6. Huang, S., Chen, C. S., and Ingber, D. E. (1998) *Mol. Biol. Cell* **9,** 3179–3193
7. Lee, K. M., Tsai, K., Wang, N., and Ingber, D. E. (1998) *Am. J. Physiol.* **274,** H76–H82
8. Dike, L. E., Chen, C. S., Mrksich, M., Tien, J., Whitesides, G. M., and Ingber, D. E. (1999) *In Vitro Cell. Dev. Biol. Anim.* **35,** 441–448
9. Polte, T., and Ingber, D. E. (2003) *Am. J. Physiol.* **286,** C518–C528
10. Folkman, J., and Moscona, A. (1978) *Nature* **273,** 345–349
11. Ezzell, R. M., Goldmann, W. H., Wang, N., Parasharama, N., and Ingber, D. E. (1997) *Exp. Cell Res.* **231,** 14–26
12. Galbraith, C. G., and Sheetz, M. P. (1998) *Curr. Opin. Cell Biol.* **10,** 566–571
13. Defilippi, P., Olivo, C., Venturino, M., Dolce, L., Silengo, L., and Tarone, G. (1999) *Microsc. Res. Tech.* **47,** 67–78
14. Ingber, D. E. (2003) *J. Cell Sci.* **116,** 1157–1173
15. Hansen, L. K., Mooney, D. J., Vacanti, J. P., and Ingber, D. E. (1994) *Mol. Biol. Cell* **5,** 967–975
16. Iwig, M., Czeslick, E., Muller, A., Gruner, M., Spindler, M., and Glaesser, D. (1995) *Eur. J. Cell Biol.* **67,** 145–157
17. Assoian, R. K. (1997) *J. Cell Biol.* **136,** 1–4
18. Huang, S., and Ingber, D. E. (2002) *Exp. Cell Res.* **275,** 255–264
19. Aplin, A. E., Short, S. M., and Juliano, R. L. (1999) *J. Biol. Chem.* **274,** 31223–31228
20. Danen, E. H., and Yamada, K. M. (2001) *J. Cell Physiol.* **189,** 1–13
21. Schwartz, M. A., and Assoian, R. K. (2001) *J. Cell Sci.* **114,** 2553–2560
22. Bohmer, R. M., Scharf, E., and Assoian, R. K. (1996) *Mol. Biol. Cell* **7,** 101–111
23. Reshetnikova, G., Barkan, R., Popov, B., Nikolsky, N., and Chang, L. S. (2000) *Exp. Cell Res.* **259,** 35–53
24. Nishi, K., Schnier, J. B., and Bradbury, M. E. (2002) *Exp. Cell Res.* **280,** 233–243
25. Sherr, C. J. (1994) *Cell* **79,** 551–555
26. Sherr, C. J., and Roberts, J. M. (1995) *Genes Dev.* **9,** 1149–1163
27. Weinberg, R. A. (1995) *Cell* **81,** 323–330
28. Sherr, C. J., and Roberts, J. M. (1999) *Genes Dev.* **13,** 1501–1512
29. Pagano, M., Tam, S. W., Theodoras, A. M., Beer-Romero, P., Del, Sal, G., Chau, V., Yew, P. R., Draetta, G. F., and Rolfe, M. (1995) *Science* **269,** 682–685
30. Zhu, X., Ohtsubo, M., Bohmer, R. M., Roberts, J. M., and Assoian, R. K. (1996) *J. Cell Biol.* **133,** 391–403
31. Kawada, M., Yamagoe, S., Murakami, Y., Suzuki, K., Mizuno, S., and Uehara, Y. (1997) *Oncogene* **15,** 629–637
32. Resnitzky, D. (1997) *Mol. Cell. Biol.* **17,** 5640–5647
33. Carrano, A. C., and Pagano, M. (2001) *J. Cell Biol.* **153,** 1381–1390
34. Kipreos, E. T., and Pagano, M. (2000) *Genome Biol.* **1,** REVIEWS3002
35. Carrano, A. C., Eytan, E., Hershko, A., and Pagano, M. (1999) *Nat. Cell. Bio.* **1,** 193–199
36. Sutterluty, H., Chatelain, E., Marti, A., Wirbelauer, C., Senften, M., Muller, U., and Krek, W. (1999) *Nat. Cell. Bio.* **1,** 207–214
37. Tsvetkov, L. M., Yeh, K. H., Lee, S. J., Sun, H., and Zhang, H. (1999) *Curr. Biol.* **9,** 661–664
38. Nakayama, K., Nagahama, H., Minamishima, Y. A., Matsumoto, M., Nakamichi, I., Kitagawa, K., Shirane, M., Tsunematsu, R., Tsukiyama, T., Ishida, N., Kitagawa, M., Nakayama, K., and Hatakeyama, S. (2000) *EMBO J.* **19,** 2069–2081
39. Hall, A. (1998) *Science* **280,** 2074–2075
40. Etienne-Manneville, S., and Hall, A. (2002) *Nature* **420,** 629–635
41. Ridley, A. J., and Hall, A. (1992) *Cell* **70,** 389–399
42. Ridley, A. J., Paterson, H. F., Johnston, C. L., Diekmann, D., and Hall, A. (1992) *Cell* **70,** 401–410
43. Nobes, C. D., and Hall, A. (1995) *Cell* **81,** 53–62
44. Chrzanowska-Wodnicka, M., and Burridge, K. (1996) *J. Cell Biol.* **133,** 1403–1415
45. Parker, K. K., Brock, A. L., Brangwynne, C., Mannix, R. J., Wang, N., Ostuni, E., Geisse, N. A., Adams, J. C., Whitesides, G. M., and Ingber, D. E. (2002) *FASEB J.* **16,** 1195–1204
46. Yamamoto, M., Marui, N., Sakai, T., Morii, N., Kozaki, S., Ikai, K., Imamura, S., and Narumiya, S. (1993) *Oncogene* **8,** 1449–1455
47. Olson, M. F., Ashworth, A., and Hall, A. (1995) *Science* **269,** 1270–1272
48. Welsh, C. F., and Assoian, R. K. (2000) *Biochim. Biophys. Acta* **1471,** M21–M29
49. Mettouchi, A., Klein, S., Guo, W., Lopez-Lago, M., Lemichez, E., Westwick, J. K., and Giancotti, F. G. (2001) *Mol. Cell* **8,** 115–127
50. Welsh, C. F., Roovers, K., Villanueva, J., Liu, Y., Schwartz, M. A., and Assoian, R. K. (2001) *Nat. Cell. Bio.* **3,** 950–957
51. Bao, W., Thullberg, M., Zhang, H., Onischenko, A., and Stromblad, S. (2002) *Mol. Cell. Biol.* **22,** 4587–4597
52. Hirai, A., Nakamura, S., Noguchi, Y., Yasuda, T., Kitagawa, M., Tatsuno, I., Oeda, T., Tahara, K., Terano, T., Narumiya, S., Kohn, L. D., and Saito, Y. (1997) *J. Biol. Chem.* **272,** 13–16
53. Weber, J. D., Hu, W., Jefcoat, S. C., Jr., Raben, D. M., and Baldassare, J. J. (1997) *J. Biol. Chem.* **272,** 32966–32971
54. Olson, M. F., Paterson, H. F., and Marshall, C. J. (1998) *Nature* **394,** 295–299
55. Hu, W., Bellone, C. J., and Baldassare, J. J. (1999) *J. Biol. Chem.* **274,** 3396–3401
56. Laufs, U., Marra, D., Node, K., and Liao, J. K. (1999) *J. Biol. Chem.* **274,** 21926–21931
57. Danen, E. H., Sonneveld, P., Sonnenberg, A., and Yamada, K. M. (2000) *J. Cell Biol.* **151,** 1413–1422
58. Assoian, R. K., and Schwartz, M. A. (2001) *Curr. Opin. Genet. Dev.* **11,** 48–53
59. Kimura, K., Ito, M., Amano, M., Chihara, K., Fukata, Y., Nakafuku, M., Yamamori, B., Feng, J., Nakano, T., Okawa, K., Iwamatsu, A., and Kaibuchi, K. (1996) *Science* **273,** 245–248
60. Kawano, Y., Fukata, Y., Oshiro, N., Amano, M., Nakamura, T., Ito, M.,

Matsumura, F., Inagaki, M., and Kaibuchi, K. (1999) *J. Cell Biol.* **147,** 1023–1038
61. Li, F., and Higgs, H. N. (2003) *Curr. Biol.* **13,** 1335–1340
62. Riveline, D., Zamir, E., Balaban, N. Q., Schwarz, U. S., Ishizaki, T., Narumiya, S., Kam, Z., Geiger, B., Bershadsky, A. D. (2001) *J. Cell Biol.* **153,** 1175–1186
63. Watanabe, N., Kato, T., Fujita, A., Ishizaki, T., and Narumiya, S. (1999) *Nat. Cell. Bio.* **1,** 136–143
64. Ishizaki, T., Morishima, Y., Okamoto, M., Furuyashiki, T., Kato, T., and Narumiya, S. (2001) *Nat. Cell. Bio.* **3,** 8–14
65. Palazzo, A. F., Cook, T. A., Alberts, A. S., and Gundersen, G. G. (2001) *Nat. Cell. Bio.* **3,** 723–729
66. Nakano, K., Takaishi, K., Kodama, A., Mammoto, A., Shiozaki, H., Monden, M., and Takai, Y. (1999) *Mol. Biol. Cell* **10,** 2481–2491
67. Sahai, E., and Marshall, C. J. (2002) *Nat. Cell. Bio.* **4,** 408–415
68. Tsuji, T., Ishizaki, T., Okamoto, M., Higashida, C., Kimura, K., Furuyashiki, T., Arakawa, Y., Birge, R. B., Nakamoto, T., Hirai, H., and Narumiya, S. (2002) *J. Cell Biol.* **157,** 819–830
69. Self, A. J., and Hall, A. (1995) *Methods Enzymol.* **256,** 3–10
70. Wilde, C., and Aktories, K. (2001) *Toxicon* **39,** 1647–1660
71. Fiorentini, C., Fabbri, A., Flatau, G., Donelli, G., Matarrese, P., Lemichez, E., Falzano, L., and Boquet, P. (1997) *J. Biol. Chem.* **272,** 19532–19537
72. Flatau, G., Lemichez, E., Gauthier, M., Chardin, P., Paris, S., Fiorentini, C., and Boquet, P. (1997) *Nature* **387,** 729–733
73. Aktories, K., Schmidt, G., and Just, I. (2000) *Biol. Chem.* **381,** 421–426
74. Numaguchi, Y., Huang, S., Polte, T. R., Eichler, G. S., Wang, N., and Ingber, D. E. (2003) *Angiogenesis* **6,** 55–64
75. Rottner, K., Hall, A, and Small, J. V. (1999) *Curr. Biol.* **9,** 640–648
76. Ren, X. D., Kiosses, W. B., and Schwartz, M. A. (1999) *EMBO J.* **18,** 578–585
77. Bishop, A. L., and Hall, A. (2000) *Biochem. J.* **348,** 241–255
78. Roovers, K., and Assoian, R. K. (2003) *Mol. Cell. Biol.* **23,** 4283–4294
79. Nobes, C. D., and Hall, A. (1999) *J. Cell Biol.* **144,** 1235–1244
80. Miralles, F., Posern, G., Zaromytidou, A. I., and Treisman, R. (2003) *Cell* **113,** 329–342
81. Copeland, J. W., and Treisman, R. (2002) *Mol. Biol. Cell* **13,** 4088–4099
82. Ingber, D. E., Prusty, D., Sun, Z., Betensky, H., and Wang, N. (1995) *J. Biomech.* **28,** 1471–1484